

FIRST RESULTS FROM CLEO-c at $E_{\text{CM}} = \Psi(3770)$

THOMAS E. COAN
Department of Physics
Southern Methodist University
Dallas, TX 75275, USA
E-mail: coan@mail.physics.smu.edu



The CLEO-c detector at CESR has begun to collect large data sets of $e^+e^- \rightarrow c\bar{c}$ events in the center-of-mass energy range $\sqrt{s} = 3 - 5$ GeV that will greatly enhance the size of the world's data sets of events produced at charm threshold. Preliminary results for the pseudoscalar decay constant f_{D^+} and absolute D-meson hadronic branching fractions from an initial integrated luminosity $\mathcal{L} = 57 \text{ pb}^{-1}$ collected at $\sqrt{s} = \Psi(3770)$ are described. These charm measurements are also relevant for B physics.

1 Leptonic D^+ Decays

Precision measurements of leptonic (and semileptonic) decays in the charm sector are vital for determining various elements of the CKM matrix that describes the mixing of quark flavors and generations induced by the weak interaction. They also can also be used to relate CKM matrix elements to mixing measurements in the $B\bar{B}$ system and to provide important experimental checks of Lattice QCD calculations. Measurements of pseudoscalar decay constants like f_{D^+} are of particular interest.

The lowest order expression for the leptonic branching fraction for the reaction $D^+ \rightarrow l^+\nu$ is given by¹

$$\mathcal{B}(D \rightarrow l\nu) = \frac{G_F^2}{8\pi} M_{D^+} m_l^2 \left(1 - \frac{m_l^2}{m_{D^+}^2}\right) f_{D^+}^2 |V_{cd}|^2 \tau_{D^+}, \quad (1)$$

where G_F is the Fermi coupling constant, M_{D^+} is the D^+ mass, m_l is the mass of the final state lepton, f_{D^+} is the parameter encapsulating the strong physics of the process, V_{cd} is the CKM matrix element encapsulating the weak physics and quantifies the amplitude for c and d quark

mixing, and τ_{D^+} is the D^+ lifetime. A measurement of $\mathcal{B}(D^+ \rightarrow \mu^+\nu)$ coupled with PDG values for V_{cd} and τ_{D^+} yields a measurement of f_{D^+} . CLEO concentrates on the reaction $D^+ \rightarrow \mu^+\nu$ since for the final state charged lepton μ^+ the branching fraction is relatively large and there are fewer final state neutrinos than for the τ^+ case.

We use 57 pb^{-1} of data collected with the CLEO-c detector at $\sqrt{s} = \Psi(3770)$. The raw data set consists of $D^0\bar{D}^0$, D^+D^- and continuum events, with possibly a small admixture of $\tau^+\tau^-$ and two-photon events. Events are divided into a “D- tag side” and a “signal side,” where the tag side is defined by attempting to fully reconstruct a candidate D^- decay into any one of the 5 modes: $D^- \rightarrow K^+\pi^-\pi^-$, $K^+\pi^-\pi^-\pi^0$, $K_S^0\pi^-$, $K_S^0\pi^-\pi^-\pi^+$, $K_S^0\pi^-\pi^0$. (Charge conjugate modes are implied in this analysis.) Charged kaons and pions are identified by using both dE/dx information from the central tracking chamber and information from the ring imaging Cherenkov (RICH) counter. Neutral pions are reconstructed using photon shower shape and location in the electromagnetic calorimeter and K_S^0 particles are reconstructed from a kinematic fit of a pair of charged pions to a displaced vertex. Cutting on the “beam constrained” D^- mass $m_D = \sqrt{E_{beam}^2 - (\sum \vec{p}_i)^2}$, where the sum is over final state particles, after fully reconstructing a D^- candidate, is also a powerful selection tool. The distribution in data for M_D as a function of D^- tag is shown in Fig. 1 where the fit curves are the superposition of Gaussian signal functions and polynomial background functions. We find 28574 ± 207 tag candidates and 8765 ± 784 background candidates.

Signal $D^+ \rightarrow \mu^+\nu$ candidates are selected after D^- tag candidates have been identified by searching for a single, oppositely charged track, presumed to be a muon. The presence of a neutrino is inferred by requiring that the measured value of the missing mass squared (MM^2) variable be near zero, where $\text{MM}^2 = (E_{beam} - E_{\mu^+})^2 - (-\vec{p}_{D^-} - \vec{p}_{\mu^+})^2$ and \vec{p}_{D^-} is the three momentum of the fully reconstructed D^- . We also require that essentially no ($< 250 \text{ MeV}$) energy in the calorimeter be unmatched to a track. Fig. 2 shows the Monte Carlo distribution of the MM^2 variable for $D^+ \rightarrow \mu^+\nu$ signal candidates as a function of D^- tag. The resolution is essentially independent of tag mode and confirmed by comparing the resolution of the MM^2 distribution for both data and Monte Carlo decays of the type $D^- \rightarrow K_S^0\pi^-$, where the same requirements are used as for the $\mu^+\nu$ search but with the extra requirement of a single detected K_S^0 . Finally, we set our signal search window to be $\pm 2\sigma$ in the $D^+ \rightarrow \mu^+\nu$ MM^2 data distribution with $\sigma = 0.028 \text{ GeV}^2$.

Fig. 3 shows the data MM^2 distribution for $D^+ \rightarrow \mu^+\nu$ candidate events after having been tagged with a fully reconstructed D^- . The insert shows 8 candidates within our search window centered about $\text{MM}^2 = 0$. The large peak at positive values of MM^2 is due to $D^+ \rightarrow K^0\pi^+$ events. Background events in our search window can arise from non $D^+ \rightarrow \mu^+\nu$ decay modes, misidentified $D\bar{D}$ events and from continuum events. The likelihood of these are evaluated using Monte Carlo simulation and the results for specific D^+ decay modes are summarized in Table 1. Backgrounds from misidentified $D\bar{D}$ decays and $e^+e^- \rightarrow \text{continuum}$ events are estimated to be 0.16 ± 0.16 and 0.17 ± 0.17 events, respectively. The total background is 1.07 ± 1.07 events, including systematic errors.

Table 1: Backgrounds from D^+ decay modes.

Mode	# of events
$D^+ \rightarrow \pi^+\pi^0$	0.31 ± 0.04
$D^+ \rightarrow K^0\pi^+$	0.06 ± 0.05
$D^+ \rightarrow \tau^+\nu$	0.36 ± 0.08
$D^+ \rightarrow \pi^0\mu^+\nu$	negligible

The branching ratio $\mathcal{B}(D^+ \rightarrow \mu^+\nu) = N_{sig}/\epsilon N_{tag}$, with the number of background subtracted

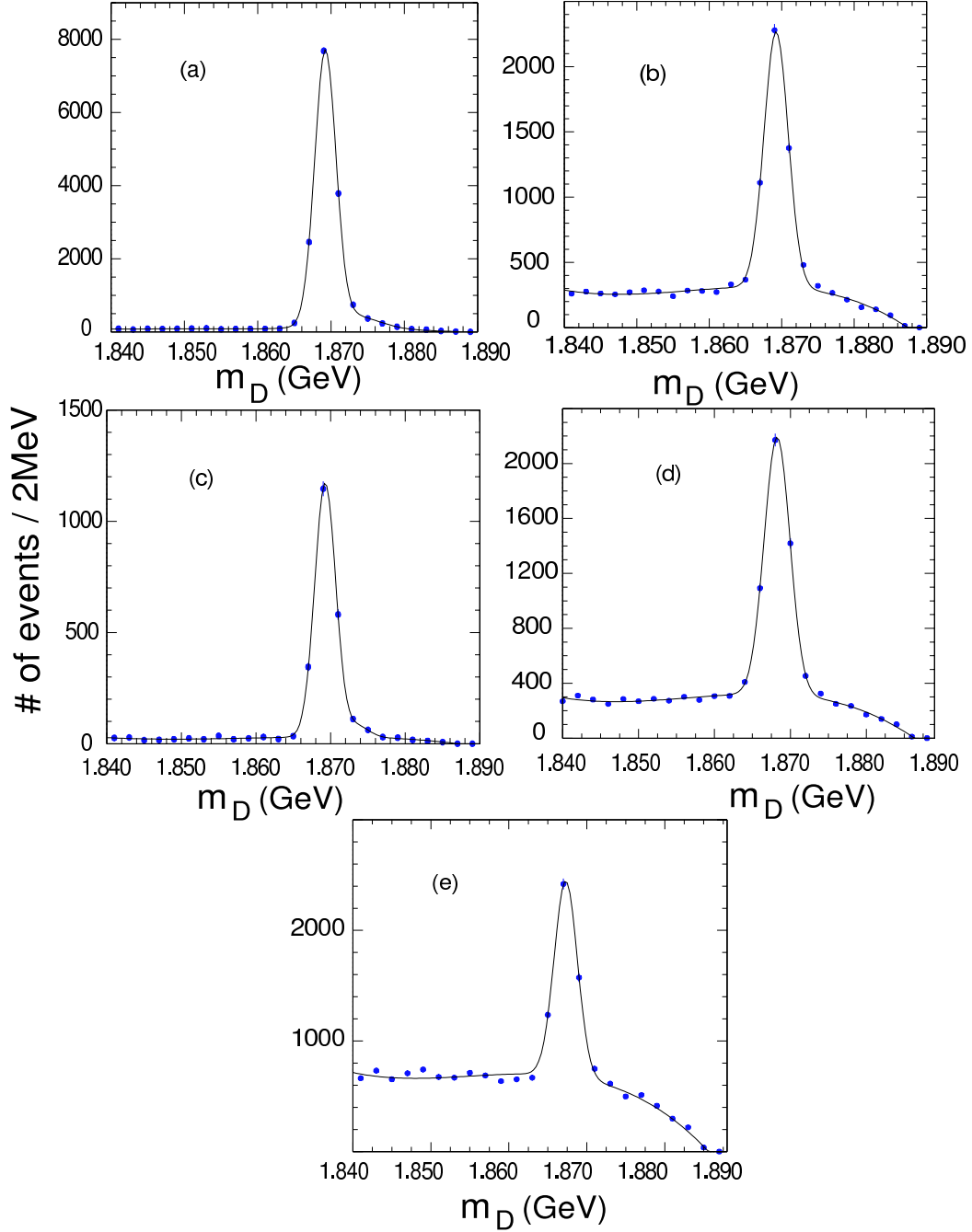


Figure 1: Distribution in data of the beam constrained mass m_D as a function of the D^- tag mode. The fit curves are superpositions of Gaussian signal functions and polynomial background functions. (a) $D^- \rightarrow K^+ \pi^- \pi^+$, (b) $D^- \rightarrow K^+ \pi^- \pi^+ \pi^0$, (c) $D^- \rightarrow K_S^0 \pi^-$, (d) $D^- \rightarrow K_S^0 \pi^- \pi^- \pi^+$, (e) $D^- \rightarrow K_S^0 \pi^- \pi^0$.

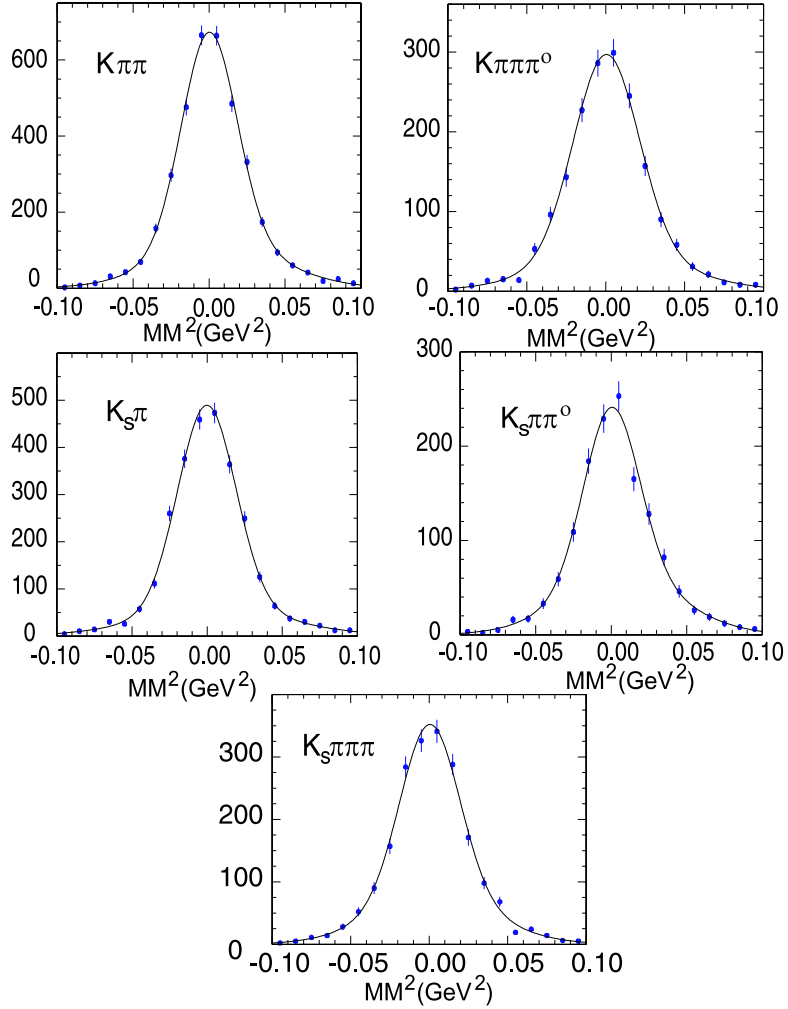


Figure 2: MM^2 distribution for simulated $D^+ \rightarrow \mu^+ \nu$ events as a function of the D^- tag mode.

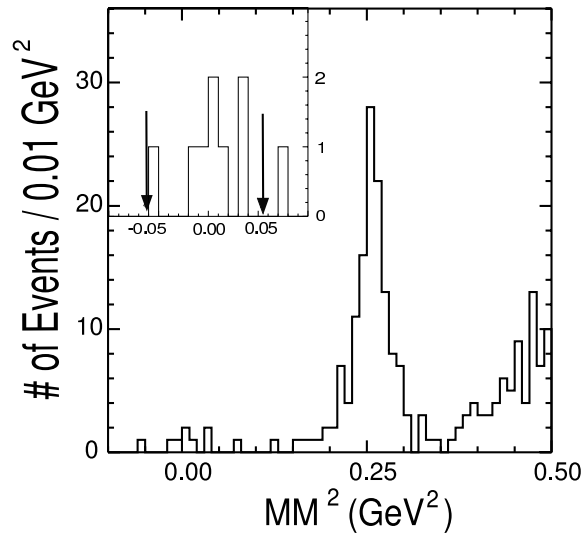


Figure 3: MM^2 distribution in data using D^- tags plus a single, oppositely charged track with no unmatched energy in the calorimeter. The insert shows 8 events inside the signal search window denoted by the arrows.

signal events $N_{sig} = 6.9 \pm 2.8$, the Monte Carlo determined single muon detection efficiency $\epsilon = 69.9\%$, and the number of D^\mp tags $N_{tag} = 28\,574 \pm 207$. The results are

$$\mathcal{B}(D^+ \rightarrow \mu^+\nu) = (3.5 \pm 1.4 \pm 0.6) \times 10^{-4} \quad \text{and} \quad f_{D^+} = (201 \pm 41 \pm 17) \text{ MeV}. \quad (2)$$

These preliminary results are the first statistically unambiguous signal for $D^+ \rightarrow \mu^+\nu$ decay, consistent with previous claims of observation² and with theoretical models³. CLEO-c intends to collect a total integrated luminosity $\mathcal{L} = 3 \text{ fb}^{-1}$ at $\sqrt{s} = \Psi(3770)$ in the next year.

2 Hadronic D-meson Branching Fractions and $\sigma(e^+e^- \rightarrow \Psi(3770) \rightarrow D\bar{D})$

The absolute branching fractions of the Cabibbo allowed decays $D^0 \rightarrow K^-\pi^+$ and $D^+ \rightarrow K^-\pi^+\pi^+$ (along with $D_s^+ \rightarrow \phi\pi^+$) are used to normalize the measurements of branching fractions for nearly all other D-meson decays. They are also used in extraction of CKM matrix elements from b and c quark decay measurements. CLEO has made preliminary measurements of 5 important D-meson branching fractions $D^0 \rightarrow K^-\pi^+$, $D^0 \rightarrow K^-\pi^+\pi^0$, $D^0 \rightarrow K^-\pi^+\pi^+\pi^-$, $D^+ \rightarrow K^-\pi^+\pi^+$ and $D^+ \rightarrow K_S^0\pi^+$, as well as the 2 production cross sections $\sigma(e^+e^- \rightarrow D^0\bar{D}^0)$ and $\sigma(e^+e^- \rightarrow D^+D^-)$ at $\sqrt{s} = \Psi(3770)$. Charged conjugate particles and decay modes are implied throughout this analysis.

The technique for branching fraction determination follows one first used by the Mark III collaboration⁴ and relies on first fully reconstructing one of the D-mesons (“single tag”) in an event to tag it as either $D^0\bar{D}^0$ or D^+D^- . Fully reconstructing the second D-meson (“double tag”) then allows the absolute branching fraction measurement of either the D^0 or the D^+ independent of the integrated luminosity or the number of $D\bar{D}$ events produced. For instance, if $N_{D\bar{D}}$ is the total number of $D\bar{D}$ events produced, then the number of single tag events N_i observed decaying via mode i with branching fraction B_i and detected with efficiency ϵ_i is $N_i = 2N_{D\bar{D}}B_i\epsilon_i$. The number of double tag events N_{ij} with the D-mesons decaying via modes i and j is then $N_{ij} = 2N_{D\bar{D}}B_iB_j\epsilon_{ij}$ for $i \neq j$ and $N_{ii} = 2N_{D\bar{D}}B_i^2\epsilon_{ii}$ otherwise. Finally, the absolute branching fraction B_i for a given mode i is found by taking the ratio of double tag events (N_{ij}) to single tag events (N_i). $B_i = (N_{ij}/N_j)(\epsilon_j/\epsilon_{ij})$ for $i \neq j$ and $B_i = 2(N_{ii}/N_j)(\epsilon_i/\epsilon_{ii})$ otherwise. Including charge conjugate particles and decay modes, we use ten single tag modes and thirteen double tag modes.

Direct use of these expressions for B_i for combining errors and measurements is problematic since N_i and N_{ij} are correlated, as are measurements of B_i for different tagging modes j . CLEO solves this problem by using a χ^2 fitting procedure that simultaneously fits branching fractions for all D^0 and D^+ decays, and for the number of $D^0\bar{D}^0$ and D^+D^- pairs produced. Statistical and systematic errors, backgrounds, efficiencies and crossfeed for different modes are accounted for directly in the fit so that experimentally measured quantities can be accounted for in a systematic fashion.

Event selection is done in a manner similar to that in the f_{D^+} analysis. Key analysis variables for the final selection of D candidates are the energy difference $\Delta E \equiv E(D) - E_0$, where $E(D)$ is the total energy of the particles of the D candidate and E_0 is the beam energy, and the square of the D candidate mass $M^2(D)c^4 \equiv E_0^2 - p^2(D)c^2$, where $p(D)$ is the magnitude of the D candidate’s three-momentum. The single tag yield in data comes from a binned maximum likelihood fit to the $M(D)$ distribution with line shape parameters determined from both Monte Carlo and data. The fit is a sum of Gaussian and Crystal Ball⁵ signal shapes plus an ARGUS background function⁶. D and \bar{D} distributions for $M(D)$ are fit together with the same signal parameters but independent backgrounds. For example, Fig. 4 shows the data $M(D)$ distribution for $D^0 \rightarrow K^-\pi^+$ on the left and $D^+ \rightarrow K^-\pi^+\pi^+$ on the right.

The double tag yield in data is extracted from an unbinned maximum likelihood fit to the two-dimensional distribution of $M(D)$ - $M(\bar{D})$ derived from double tag candidate events. Again,

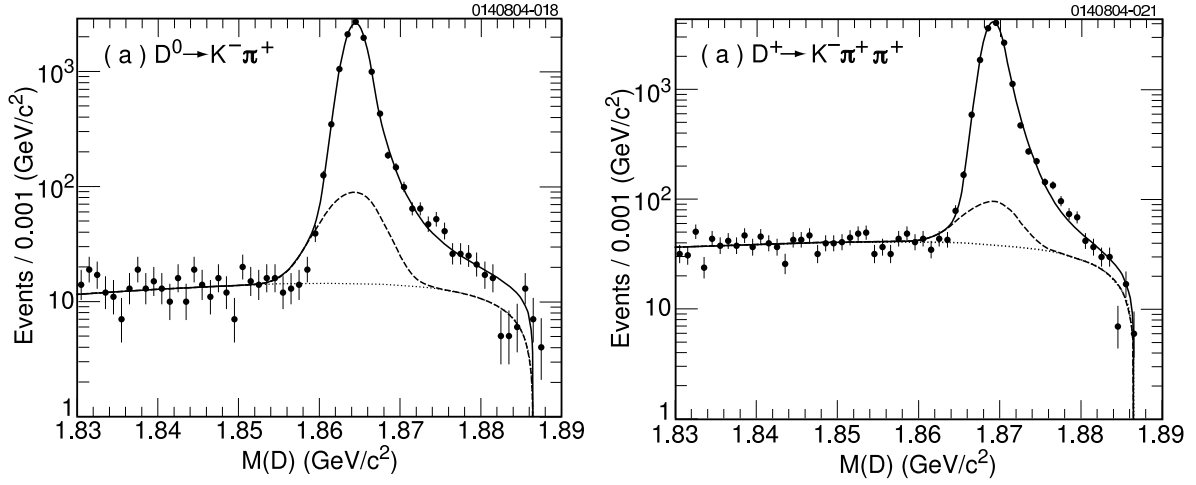


Figure 4: $M(D)$ distribution in data for single tag candidates for the decay mode $D^0 \rightarrow K^- \pi^+$ (left) and $D^+ \rightarrow K^- \pi^+ \pi^+$ (right). The data are dots and the lines are the fit showing the Gaussian and Crystal Ball signal functions and ARGUS background function.

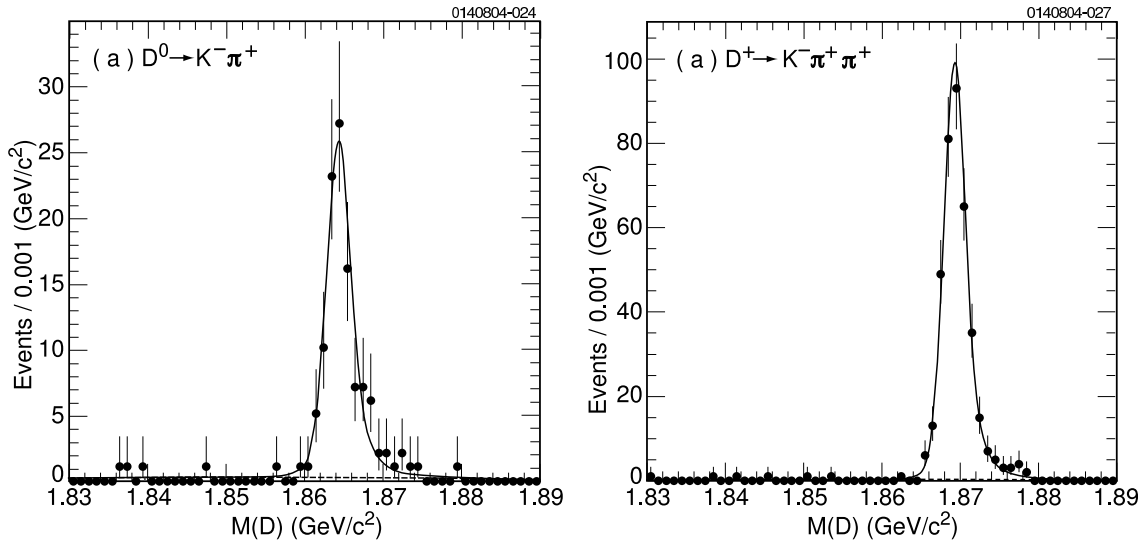


Figure 5: Projection of the double tag $D^0\text{-}\bar{D}^0$ candidate masses onto the $M(D)$ axis for the decay mode $D^0 \rightarrow K^- \pi^+$ (and its charge conjugate mode) is shown in the left hand plot while the right hand plot shows a similar projection of $D^+\text{-}D^-$ candidate masses for the decay mode $D^+ \rightarrow K^- \pi^+ \pi^+$ (and its charge conjugate mode).

shape parameters are determined from a combination of Monte Carlo and data events. As an example, Fig. 5 shows the projection of the fit onto the $M(D)$ axis for the case when the D -mesons are reconstructed as $D^0 \rightarrow K^- \pi^+$ and $\bar{D}^0 \rightarrow K^+ \pi^-$ (left-hand side). The right-hand side shows a similar projection for the case $D^+ \rightarrow K^- \pi^+ \pi^+$ and $D^- \rightarrow K^+ \pi^- \pi^-$.

The branching fraction fit for the D -meson branching fractions listed above as well as $N_{D^0 \bar{D}^0}$ and $N_{D^+ D^-}$, uses event yields and efficiencies for ten single tag and thirteen double tag modes. Crossfeed and backgrounds are accounted for in the fit. The χ^2 of the fit is 8.9 for 16 degrees of freedom (confidence level = 92%) and the fit results are shown in Table 2. The branching fractions are consistent with, but somewhat higher than, the current PDG values. In nearly all cases, our statistical error for the branching fractions and their ratios is less than the statistical error of the individual measurements comprising the PDG average. Cross sections are extracted using our current integrated luminosity $\mathcal{L} = 57 \text{ pb}^{-1}$. The statistical and systematic errors of these preliminary results should drop markedly when CLEO accumulates its anticipated 3 fb^{-1} of integrated luminosity.

Table 2: Fit results for branching fractions and $D\bar{D}$ pair yields, and inferred production cross sections. First error is statistical and second is systematic.

Parameter	Fitted/Inferred Value
$\mathcal{B}(D^0 \rightarrow K^- \pi^+)$	$(3.92 \pm 0.08 \pm 0.23)\%$
$\mathcal{B}(D^0 \rightarrow K^- \pi^+ \pi^0)$	$(14.3 \pm 0.3 \pm 1.0)\%$
$\mathcal{B}(D^0 \rightarrow K^- \pi^+ \pi^- \pi^+)$	$(8.1 \pm 0.2 \pm 0.9)\%$
$\mathcal{B}(D^+ \rightarrow K^- \pi^+ \pi^+)$	$(9.8 \pm 0.4 \pm 0.8)\%$
$\mathcal{B}(D^+ \rightarrow K_S^0 \pi^+)$	$(1.61 \pm 0.08 \pm 0.15)\%$
$N_{D^0 \bar{D}^0}$	1.98×10^5
$N_{D^+ D^-}$	1.48×10^5
$\sigma(e^+ e^- \rightarrow \Psi(3770) \rightarrow D^0 D^0)$	$3.47 \pm 0.07 \pm 0.15 \text{ nb}$
$\sigma(e^+ e^- \rightarrow \Psi(3770) \rightarrow D^+ D^-)$	$2.59 \pm 0.11 \pm 0.11 \text{ nb}$
$\sigma(e^+ e^- \rightarrow \Psi(3770) \rightarrow D\bar{D})$	$6.06 \pm 0.13 \pm 0.22 \text{ nb}$

Acknowledgments

The author would like to thank the conference organizers for the invitation and the stimulating environment, the U.S. Department of Energy for its support under contract DE-FG03-95ER40908, and W.M. Sun for useful discussion.

References

1. N. Barik and P.C. Dash, *Phys. Rev.* **D47**, 2788 (1993).
2. G. Rong, XXXIXth Rencontres de Moriond, Electroweak Interactions and Unified Theories, 21-28 March 2004, La Thuile, Italy [hep-ex/0406027].
3. L. Lellouch *et al.*, *Phys. Rev.* **D45**, 094501 (2001); Z.G. Wang *et al.*, [hep-ph/0403259]; L. Salcedo *et al.*, *Braz. J. Phys.* **34**, 297 (2004) [hep-ph/0311008]; S. Narison, [hep-ph/0202200]; A. Penin *et al.* *Phys. Rev.* **D65**, 054006 (2002); D. Ebert *et al.*, *Mod. Phys. Lett.* **A17**, 803 (2002); J. Amundson *et al.*, *Phys. Rev.* **D47**, 3059 (1993)[hep-ph/9207235].
4. Mark III collaboration, R.M. Baltrusaitis *et al.* *Phys. Rev. Lett.* **56**, 2140 (1986).
5. T. Skwarnicki, DESY Report No. DESY F31-86-02.
6. ARGUS collaboration, H. Albrecht *et al.*, *Phys. Lett. B* **241**, 278 (1990).